CHEMISTRY
AN ASIAN JOURNAL
www.chemasianj.org

Accepted Article

Title: Alkene-azide 1,3-dipolar cycloaddition as a trigger for ultrashort peptide hydrogel dissolution

Authors: Sumit Dadhwal, Jessica M Fairhall, Shailesh K Goswami, Sarah Hook, and Allan Bernard Gamble

To be cited as: *Chem. Asian J.* 10.1002/asia.201801184

Link to VoR: http://dx.doi.org/10.1002/asia.201801184

A Journal of
ACES Asian Chemical Editorial Society

A sister journal of Angewandte Chemie and Chemistry – A European Journal

WILEY-VCH

10.1002/asia.201801184

WILEY-VCH

FULL PAPER

Alkene-azide 1,3-dipolar cycloaddition as a trigger for ultrashort peptide hydrogel dissolution

Sumit Dadhwal,[a] Jessica M. Fairhall,[a] Shailesh K. Goswami,[b] Sarah Hook[a] and Allan B. Gamble*[a]

Abstract: An alkene-azide 1,3-dipolar cycloaddition between *trans*-cyclooctene (TCO) and an azide-capped hydrogel that promotes rapid gel dissolution is reported. Using an ultrashort aryl azide-capped peptide hydrogel (PhePhe), we have demonstrated proof-of-concept where upon reaction with TCO, the hydrogel undergoes a gel-sol transition via 1,2,3-triazoline degradation and 1,6-self-immolation of the generated aniline. The potential application of this as a general trigger in sustained drug delivery is demonstrated through release of encapsulated cargo (doxorubicin). Administration of TCO resulted in 87% of the cargo being released in 10 h, compared to 13-14% in the control gels. This is the first example of a potential bioorthogonal-triggered hydrogel dissolution using a traditional click-type reaction. This type of stimulus could be extended to other aryl azide-capped hydrogels.

Introduction

Physical cross-linking of ultrashort peptides via non-covalent forces which include electrostatic, hydrogen bonding, π-π stacking, van der Waals and hydrophobic interactions, allows for the formation of tangled hydrogel networks.[1] Easy preparation of ultrashort peptides combined with their biocompatibility, biodegradability, and non-immunogenic properties, makes their application in drug delivery,[2] biosensing,[3] wound healing,[4] cell culture[5] and cancer cell growth inhibition[6] very appealing. In particular, the ease of synthesis for ultrashort peptide sequences bearing a hydrophobic aromatic group at their N- or C-terminus[7] has provided hydrogels that are considered promising candidates for drug delivery systems. The aromatic capping group can induce gelation via hydrophobic and π-π stacking interactions[8] and it is typically conjugated to a short phenylalanine sequence at the N-terminus. Commonly used hydrophobic moieties which favor self-assembled nanofiber networks include Fmoc,[9] pyrene,[10] or naphthalene.[11] Recently, stimuli-sensitive ultrashort peptide hydrogels have been developed, further increasing their applications in drug delivery.[1b,12]

The replacement of simple N-terminus aromatic hydrophobic units with stimuli-responsive moieties has provided peptide hydrogels capable of triggered gel breakdown via stimuli such as pH, enzyme hydrolysis and reduction, temperature and ionic strength.[1b] In these examples, the basic principle for gel breakdown is the removal of the hydrophobic capping group following the stimulus, which destroys the delicate hydrophobic–hydrophilic balance in the gel network resulting in a gel-sol transition. Based on this strategy, more recent examples have investigated ultrashort peptide hydrogels that are responsive to reactive oxygen species (ROS) such as hydrogen peroxide (H_2O_2), for example via aryl boronates at the N-terminus,[13] or a thiazolidinone group at the C-terminus.[2c] In another example, Sun et al. used *p*-azidobenzyl carbamate as the N-terminus protecting group which was reduced to the aniline by hydrogen sulfide (H_2S), followed by subsequent 1,6-self-immolation to release the free peptide.[14] However, generating stable peptide hydrogels which only respond in a highly specific way to endogenous (e.g. pH, reduction, ROS) or exogenous stimuli (e.g. light) remains as a significant challenge in the drug delivery field.[15] Furthermore, the complexity of a biological system makes it difficult for smart materials such as ultrashort peptide hydrogels to detect low levels (nM to μM) of biologically relevant stimuli, for example H_2S which is only present in very low and highly localised levels.[16] Therefore, there is an urgent need to develop better endogenous and exogenous stimuli-responsive triggers that can be used in peptide hydrogels.

Bioorthogonal chemical reactions that can be carried out in biological and physiological systems[17] have been widely utilised in biological imaging,[18] prodrug/protein decaging strategies[19] and drug delivery.[20] More recently, click reactions such as the strain-promoted azide-alkyne cycloaddition (SPAAC), oxime ligation and the inverse-electron-demand Diels-Alder (IEDDA) reaction between a *trans*-cyclooctene (TCO) and tetrazine have been utilised as a cross-linker for hydrogels[21] and as reservoirs for activation of TCO-functionalised prodrugs (via an IEDDA reaction).[22] Truong and co-workers recently used bioorthogonal reactions to promote the formation of hydrogels capable of controlled release by visible and UV light.[23] While these strain-promoted bioorthogonal reactions have been used to form polymeric hydrogels or activate prodrugs, the use of such chemical reactions to directly promote gel-sol transition has, to the best of our knowledge, not been reported. We recently reported a bioorthogonal strain-promoted 1,3-dipolar cycloaddition between a *trans*-cyclooctenol (TCO) and an azide that was used for prodrug activation;[24,25] a reaction that could be exploited for peptide gel-sol transition purposes. Herein we report the first example of a bioorthogonal reaction that directly triggers hydrogel dissolution via a click-type reaction. As a proof-of-concept, a simple *N*-azido-capped phenylalanine-phenylalanine (PhePhe) hydrogel **1** was utilised (Scheme 1).

[a] S. Dadhwal, J. M. Fairhall, Prof. S. Hook and Dr A. B. Gamble.
School of Pharmacy, University of Otago
E-mail: allan.gamble@otago.ac.nz
[b] Dr. S. K. Goswami
Department of Chemistry
University of Otago

Supporting information for this article is given via a link at the end of the document.

10.1002/asia.201801184

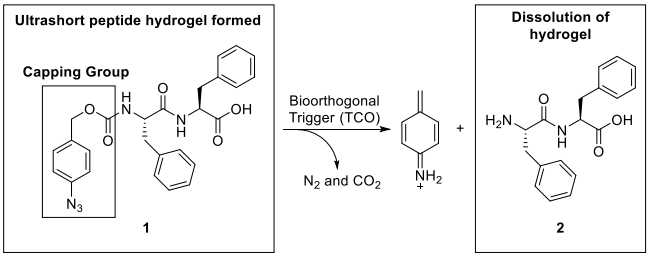

Scheme 1 Proposed gel–sol transition of a *p*-azidobenzyl carbamate-PhePhe dipeptide hydrogel **1** via a bioorthogonal chemical stimulant (TCO).

Results and Discussion

The synthesis of the *p*-azidobenzyl carbamate-PhePhe **1** was achieved through formation of *p*-azidobenzyl alcohol **4**, which was subsequently converted to the activated succinate ester **5** by reaction with *N*,*N*′-disuccinimidyl carbonate (DSC). Reaction of the activated ester with the dipeptide PhePhe **2** under alkaline conditions provided **1** (Scheme 2).

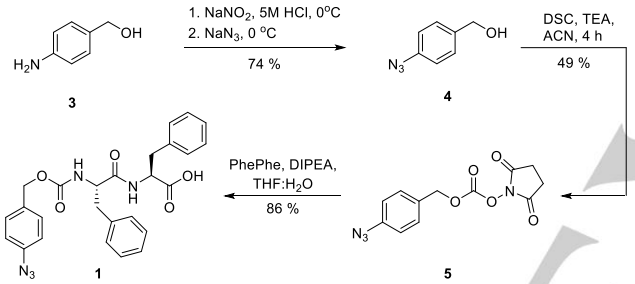

Scheme 2 Synthesis of the *p*-azidobenzyl carbamate-PhePhe dipeptide **1**.

To promote hydrogel formation of **1**, the solvent switch method was used by dissolving PhePhe-dipeptide **1** in DMSO followed by addition of water or buffer (final DMSO conc. 5%). The water/DMSO gel (final pH 3.4) was used for subsequent TEM/SEM imaging and gel rheology studies, while in depth proof-of-principle release studies were conducted using hydrogels at 0.5 wt% in PBS (final DMSO conc. 5%; pH = 5.7). The critical gel concentration for dipeptide **1** in water (5% DMSO) was determined by the tube inversion method to be 0.5 wt% with a pH of 3.4 (Figure 1A). The mechanical properties of the gel (water/DMSO) were investigated using rheology (Figure 1B), with the storage (*G*′) and loss (*G*″) moduli measured using dynamic frequency sweeps at a fixed strain of 0.5% in the frequency range 0.1 to 100 rad s^{-1}. Stable gel formation was confirmed by the higher *G*′ value of the gel and long entangled fibres were confirmed by transmission electron microscopy (TEM) and scanning electron microscopy (SEM) (Figure 1C, 1D and Figure S1). The TEM time series experiments showed that gel formation started immediately (within 5 sec), firstly via the formation of vesicles (Figure S2A), and then initial fibres (Figure S2B). The fibres then became entangled and formed a stable viscous hydrogel (Figure 1C, 1D).

Hydrogel formation was also examined under different pH conditions in a PBS or acetate buffer that was adjusted to the desired pH using HCl or NaOH (pH 7.4, 6.5 and 4.5) (Figure S3). Stable hydrogels were confirmed by the inversion method; white/cloudy gel at pH 4.5 (acetate buffer), transparent gel at pH 6.5 and 7.4 (Figure S3). To compare the morphology of the hydrogels under neutral pH (7.4) to that under acidic pH (3.7), a hydrogel of **1** (0.5 wt%) was prepared in water/DMSO (adjusted to pH 7.4 with NaOH) and analysed by TEM (Figure S4). The TEM image showed that at neutral pH, the hydrogel prepared from dipeptide **1** maintained the long entangled fibres observed under more acidic pH (Figure 1C/1D).

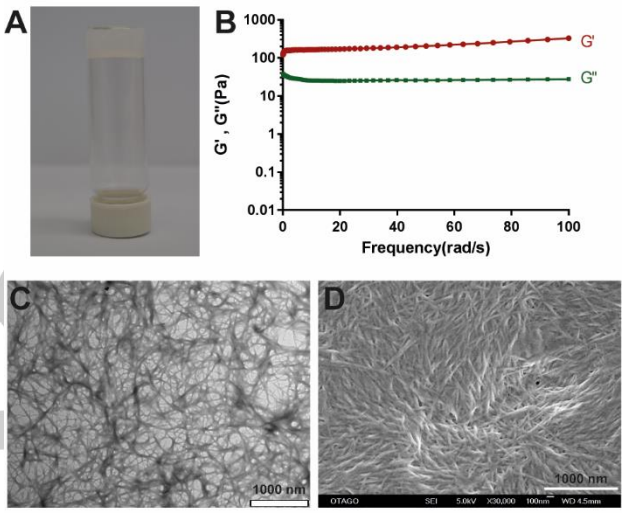

Figure 1 Characterisation data for dipeptide hydrogel **1**. (A) Hydrogel at 0.5 wt% in water and 5% DMSO. (B) Rheological data for 0.5 wt% gel measured at 25 °C. (C) TEM image of dipeptide gel **1** (scale bar = 1000 nm). (D) SEM image of dipeptide gel **1** (white scale bar = 1000 nm).

trans-Cyclooctene triggered gel-sol transition

Next we investigated the dissolution of hydrogel **1** using TCO as the bioorthogonal trigger (Scheme 3). The same mechanism as for prodrug activation[24,25] was proposed for hydrogel dissolution. In the first step, 1,3-dipolar cycloaddition between TCO and azide **1** is expected to result in the formation of 1,2,3-triazoline **6**, which is relatively unstable under aqueous conditions and converted to the imine **7** via extrusion of diatomic nitrogen (expected to result in visual bubbles within the gel). Hydrolysis of imine **7** would provide aldehyde **9** and aniline-capped dipeptide **8**, that undergoes a rapid (seconds-to-minutes) 1,6-self-immolation, releasing dipeptide **2** and an azaquinone-methide which reacts with water to generate an aminobenzyl alcohol **10**.

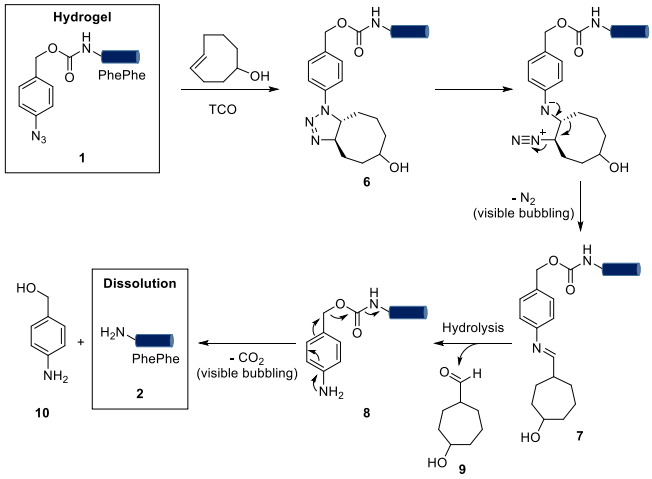

Scheme 3 Proposed mechanism for gel-sol transition by a 1,3-dipolar cycloaddition using **1** as a model system.

Initially we examined the visible breakdown of the gel in water (pH 3.4) upon addition of 1, 5 and 10 mM TCO. Inversion of the vial prior to TCO addition indicated the formation of a viscous white hydrogel (Figure 1A), which after addition of TCO (5 or 10 mM) became a free flowing yellow liquid over time, with white precipitates suspended in the solution (Figure 2A). TEM analysis of the TCO-triggered gel provided further macroscopic evidence for the breakdown of gel (Figure 2B), with the well-defined fibrous network of dipeptide **1** before the trigger absent (Figure 2B *c.f.* Figure 1C). Adding 10 mM TCO to the gel resulted in complete visual dissolution by 4 h (Figure S5A), whereas with 5 mM TCO it took approx. 10 h to achieve the same level of dissolution. The gel with 1 mM TCO did not show any sign of dissolution, even after 12 h. The control gel (PBS only added) also did not show any sign of gel-sol transition. Visual dissolution of the hydrogel at pH 4.5 (acetate buffer), 6.5 (PBS), 7.4 (PBS) in the presence of 10 mM TCO also resulted in a gel-sol transition within 2-4 hours (Figure S3).

Time-dependent rheology experiments were conducted on the water/DMSO hydrogels (pH 3.4) to examine the change in gel strength during the gel-sol transition (Figure S6). The results demonstrate a decrease in storage (G') and loss (G'') moduli following the addition of 10 mM TCO (Figure S6). There is a gradual decrease in G' and G'' over the first two hours, and by 4 hours, both G' and G'' have decreased by an order of magnitude, supporting the time reported for visual gel-sol transition. This suggests that following the 1,3-dipolar cycloaddition of **1** with 10 mM TCO, there is a gradual loss in mechanical strength of the hydrogel due to triazoline/imine hydrolysis and self-immolation to **2**, with significant gel-sol transition evident at 4 hours.

To ensure that the 1,3-dipolar cycloaddition was essential for dissolution of hydrogel **1**, and it was not a simple diffusion of the hydrophobic TCO into the fibrous network causing disruption of the π-π stacking interactions, 1 mL of gel **1** (0.5 wt%) was incubated with 10 mM of the low-strain *cis*-cyclooctenol (CCO) in PBS (0.5 mL). We have previously shown that the low-strain CCO does not undergo a 1,3-dipolar cycloaddition with aryl azides at 37 °C,[24] and as expected, after 24 h at 37 °C the gel **1** did not show any visible signs of dissolution (Figure S5B).

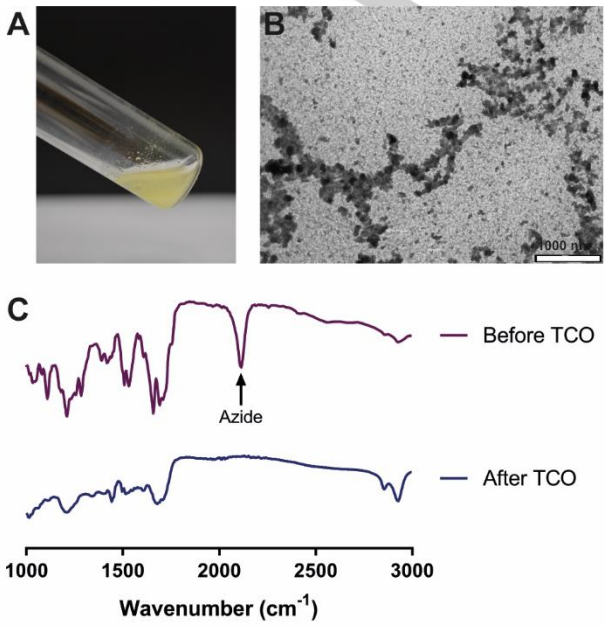

Figure 2 Characterisation of dipeptide hydrogel **1** after addition of the TCO trigger (10 mM) (A) Visual appearance of gel. (B) TEM image demonstrating the loss of fibrous network (*c.f.* Figure 1C). (white scale bar = 1000 nm). (C) Infrared spectrum of hydrogel **1** before and after addition of the TCO trigger showing the presence and then subsequent disappearance of azide.

Infrared (IR) spectroscopy also confirmed that the 1,3-dipolar cycloaddition of TCO with aryl azide had occurred, with the strong asymmetric N≡N azide peak at ~2100 cm^{-1} absent after incubating with TCO (10 mM) and analysing the lyophilised sample (Figure 2C). High resolution mass spectral (HRMS) analysis of a sample hydrogel prepared in buffer and dissolved by the addition of TCO in PBS (pH 5.7) indicated that all of the azide-capped dipeptide **1** had reacted with TCO and released the capping group; confirmed via the absence of a peak corresponding to the molecular ion of **1**, and the presence of a peak at *m/z* 311.1420 (Figure S7) in the negative ion HRMS (ESI-) assigned as the M-H ion for dipeptide **2**. The expected 4-aminobenzyl alcohol **10** that is generated as a by-product of the 1,6-self-immolation of the capping group was not observed under HRMS-ESI positive or negative conditions. Notably, a sample of commercially available 4-aminobenzyl alcohol **10** failed to produce a *m/z* ion under the HRMS-ESI positive and negative conditions.

In the absence of a conclusive ion for 4-aminobenzyl alcohol **10**, further evidence for the proposed imine hydrolysis mechanism was provided via the gel-sol transition at various pH. Gels were prepared in buffer at a final pH of 7.4 and 4.5 (*vide supra*) and TCO (10 mM) was added. The samples were then lyophilized and their HRMS (ESI-) spectra recorded (Figure S8). As expected, each sample showed evidence of an ion that matched the expected *m/z* ratio of dipeptide **2** (around *m/z* 311.14). Interestingly, the gel at pH 7.4 had an additional two peaks at *m/z*

10.1002/asia.201801184

584.2736 and 435.2270, which could be assigned to imine **7** (trace amounts) and the imine **11** that forms upon reaction of dipeptide **2** with the aldehyde **9** (Scheme 4). Imine **11** (*m/z* 435.2270) can only be generated upon hydrolysis of the initial imine **7**, and subsequent 1,6-self-immolation of **8**. The peaks for imines **7** and **11** were not evident in gels that were formed and triggered under more acidic pH (pH = 5.7, 4.5), most likely due to the reduced nucleophilicity of the amino group on the N-terminus of PhePhe **2**, and/or the acid-sensitivity of the newly formed imine bond. In combination with the visual and spectroscopic data, the HRMS data at neutral and acidic pH provides supporting, albeit indirect evidence that the dissolution mechanism proceeds via the proposed imine **7** in Scheme 3.

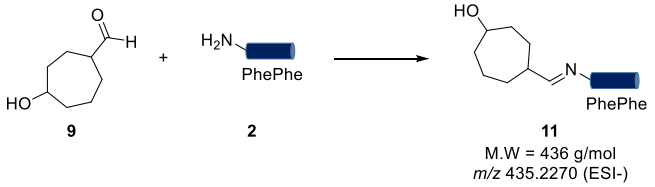

Scheme 4 Proposed formation of imine **11** following imine hydrolysis of **7** and 1,6-self-immolation of **8**. Imine **11** was identified by HRMS (ESI-).

Next the rate of 1,3-dipolar cycloaddition between TCO and **1** was measured. Ideally, the rate for the cycloaddition would have been measured with the preformed hydrogel network, however, as the gel-sol process does not occur immediately (i.e. triazoline/imine degradation is delayed), we could not easily take early aliquots of the reaction for HPLC measurement. Therefore, to estimate the rate of the 1,3-dipolar cycloaddition for hydrogel **1**, we monitored the reaction of azido-dipeptide **1** and TCO in solution phase (MeCN:PBS; 1:1). Using HPLC (Figure S9 and S10), the disappearance of **1** (R_T = 7.9 min) was measured under pseudo first-order conditions (at 254 nm), and the second-order rate constant was determined as 0.018 $M^{-1}s^{-1}$, a rate comparable to our previously reported bioorthogonal prodrug activation.[24,25] In the absence of HPLC data on the gel-sol transition itself, we performed a time-dependent analysis of the 1,3-dipolar cycloaddition using IR spectroscopy. The IR results demonstrated that after 1 hour a small amount of azide was yet to react with TCO (presence of azide peak evident), but by 4 hours all of the azide in the gel had been consumed (Figure S11).

Triggered release of cargo during gel-sol transition

Next, the ability of our reaction to trigger the release of cargo from hydrogel **1** was examined. Using doxorubicin as a model cargo/drug, the ability of the gel to encapsulate and then release the drug from its fibrous network using TCO as the bioorthogonal trigger was determined (Figure 3). Doxorubicin (0.17 mM; 100 μg/mL) was encapsulated in 1 mL of the dipeptide hydrogel **1** (pH 6.1). The gel was left undisturbed for 20 min and then 0.5 mL of PBS containing 5 mM TCO trigger was added to the gel, and incubated at 37 °C. As control experiments, 0.5 mL PBS (pH 7.4) with no TCO and 0.5 mL of PBS containing CCO was added to hydrogel **1**. At the indicated times in Figure 3, 0.5 mL of sample was taken and replaced with a fresh 0.5 mL PBS aliquot containing 5 mM TCO (5 mM CCO or PBS only for controls) and incubation continued at 37 °C. The release of doxorubicin from the hydrogel was analysed by UV-absorbance (485 nm) and quantified using a doxorubicin standard curve (Figure S12). The gel with TCO had a cumulative doxorubicin release of 87% in 10 h, whereas the hydrogels containing CCO or PBS, resulted in 13% and 14% of doxorubicin being released in 10 h, respectively.

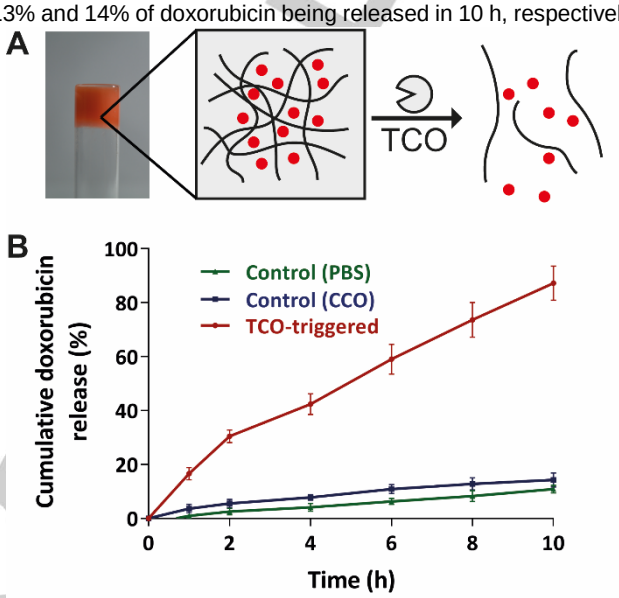

Figure 3 (A) Hydrogel **1** showing encapsulation of doxorubicin, and cartoon representation of expected gel-sol transition and subsequent release of doxorubicin (red dots). (B) Cumulative release of doxorubicin from **1** incubated with 5 mM TCO, 5 mM CCO or PBS only. Absorbance was measured at 485 nm. Error bars represent the SD for triplicate experiments.

Cytotoxicity of dipeptide 1 and TCO

The biocompatibility of dipeptide **1** (added as a solution in DMSO) was tested using B16F10 melanoma cells and Madin-Darby Canine Kidney (MDCK) cells (Figure 4). Various concentrations of **1** (10 μM to 4 mM) were incubated with the melanoma and kidney cells for 24 h, and cytotoxicity was measured by a resazurin assay (See experimental section). The cell viability was compared to the control cells which did not contain **1** (0 μM; 100% viable). There was no significant decrease in cell viability at concentrations of **1** less than 200 μM and 500 μM in melanoma and kidney cells, respectively. At higher concentrations, cytotoxicity was evident, with approx. 50% cell viability at 250 μM (melanoma) and 1 mM (kidney). Interestingly, higher cytotoxicity was observed in the melanoma cell lines, possibly due to their higher intracellular uptake of dipeptide **1**. The cytotoxicity of the trigger (TCO) towards the MDCK cells was lower than for the melanoma cell lines (Figure S13). Overall, the azide-functionalized dipeptide **1** and TCO have good biocompatibility at lower concentrations. However, a hydrogel with lower critical gel concentration and a more responsive gel-sol transition in response to the stimulus/trigger would enable the concentration of the dipeptide and TCO trigger to be lowered, potentially reducing cytotoxicity of the system. Work investigating

10.1002/asia.201801184

novel hydrogels with lower critical gel concentrations and higher sensitivity to TCO is ongoing in our laboratory.

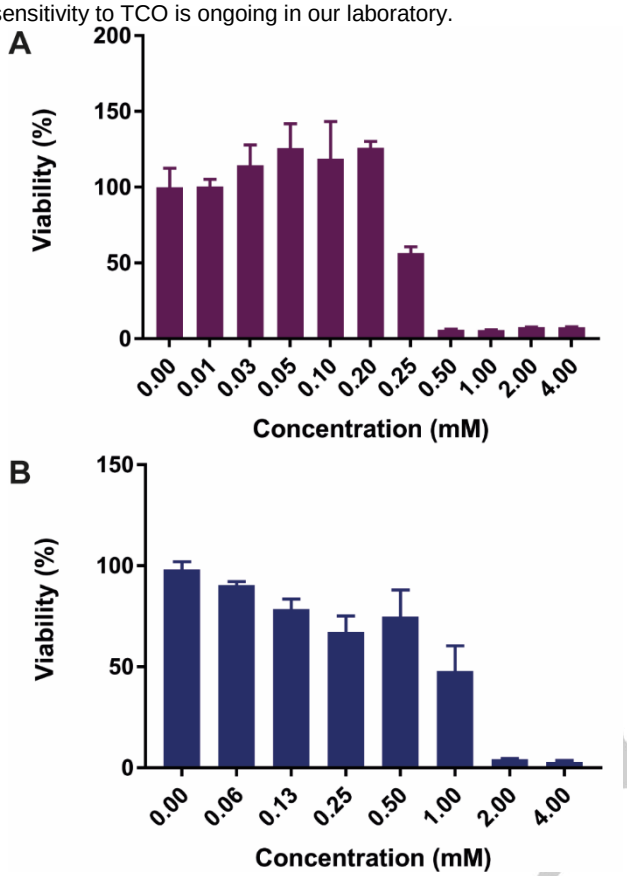

Figure 4 Cell viability study for azido-PhePhe **1** against (A) B16F10 melanoma and (B) MDCK kidney cells. Error bars represent the SD for triplicate experiments.

Conclusion

In summary, we have reported the first use of a strain-promoted alkene-azide 1,3-dipolar cycloaddition that can trigger the dissolution of a hydrogel. As proof-of-principle, a *p*-azidobenzyl carbamate-PhePhe dipeptide **1** was selected as a simple model system. Dipeptide **1** formed a stable cross-linked network in water or PBS, that upon addition of the bioorthogonal reagent (TCO), underwent a rapid 1,3-dipolar cycloaddition to promote the gel-sol transition process. The control experiment with CCO, the low strain isomer of TCO, did not result in dissolution of gel **1**, indicating that 1,2,3-triazoline generation followed by release of dipeptide **2** is required for gel-sol transition in this system. To demonstrate that the bioorthogonal-triggered dissolution could have applications in sustained cargo delivery systems, we encapsulated doxorubicin in hydrogel **1** and quantified its release after introduction of TCO. The amount of doxorubicin released was 87% over 10 h compared to only 13% and 14% in the non-triggered control experiments. We are currently examining the bioorthogonal trigger with other peptide hydrogels. This will enable us to improve hydrogel stability, biocompatibility, sensitivity to TCO, and ultimately gain control over the rate of TCO-promoted gel-sol transition.

Experimental Section

General experimental and synthesis

All chemicals were purchased from commercial suppliers and used without purification unless otherwise stated. 5-Hydroxy-1-cyclooctene (*cis*-cyclooct-4-enol) was purchased from Carbosynth Limited, UK. Silver nitrate-impregnated silica gel was purchased from Silicycle (SiliaBond® Silver Nitrate, 40-63µm, 60Å). Diphenylalanine was purchased from AK Scientific, USA. Doxorubicin hydrochloride (DOX) was purchased from Lancrix Chemicals, Shanghai, China. All other reagents were purchased from Sigma-Aldrich or AK Scientific.

^{1}H and ^{13}C NMR spectra were recorded on a 400 MHz Varian MR spectrometer. Chemical shifts are reported as δ in parts per million (ppm) and coupling constants are reported as *J* values in Hz. High resolution electrospray ionization mass spectra (ESI-MS) were recorded on a microTOF$_Q$ mass spectrometer. Photochemical reactions were performed in a Southern New England Ultraviolet Company Rayonet® reactor model RPR-100, equipped with eight RPR-2537 Å lamps. Reactions were performed in either the RQV-118 or RQV-218 quartz reaction vessels supplied by Southern New England Ultraviolet Company. Rheology measurements were performed using a cone- and plate geometry on Oscillatory HR 3 rheometer (TA instrument). The synthesis of 4-azidobenzyl alcohol[26] **4** and *trans*-cyclooct-4-enol (TCO)[27] were synthesised according to literature procedures (ESI, Section 1).

4-Azidophenyl succinic carbonate 5. Synthesised using a previously reported literature procedure.[13] To a solution of N,N′-disuccinimidyl carbonate (DSC) (2.1 g, 8.19 mmol) in dry acetonitrile (15 mL), was added benzyl alcohol **4** (0.500 g, 3.36 mmol) and triethylamine (TEA) (0.65 g 6.4 mmol). The mixture was stirred under nitrogen at 0 °C for 30 min and then room temperature for an additional 4 h. The reaction mixture was monitored by TLC and after complete consumption of starting material, solvent was evaporated under vacuum. The crude reaction mixture was dissolved in CH_2Cl_2 (50 mL) and washed with water (2 x 100 mL). The organic layer was collected and dried over $MgSO_4$. The crude product was loaded on silica gel and subjected to flash silica gel column chromatography (30% ethyl acetate:hexanes) to afford the title compound as a white solid (0.480 g, 49 %). ^{1}H NMR ($CDCl_3$, 400 MHz): δ 7.37 (d, *J* = 8.4 Hz, 2 H); 7.04 (d, *J* = 8.4 Hz, 2 H); 5.26 (s, 2 H); 2.82 (s, 4 H). ^{13}C NMR ($CDCl_3$, 100 MHz): 168.7, 151.6, 141.1, 130.4, 129.9, 119.4, 72.2, 25.4.

(4-Azidobenzyloxycarbonyl)-L-phenylalanyl-L-phenylalanine 1. Synthesised using a previously reported literature procedure.[13] To a solution of 4-azidophenyl succinic carbonate **5** (0.200 g, 0.69 mmol) in THF (12 mL) was added L-Phe-L-Phe **2** (0.320 g, 1.03 mmol) and DIPEA (0.133 g, 1.03 mmol) followed by addition of deionised water (3 mL). The reaction was stirred for 2 h at room temperature. The reaction was monitored by TLC and after completion of the reaction, the THF was evaporated under vacuum and the aqueous mixture was acidified (pH 2-3) with 5% citric acid solution. The acidified reaction mixture was extracted with ethyl acetate (3 x 25 mL) and the combined organic layer was washed with water. The organic layer was dried over $MgSO_4$ and filtered. The filtrate was concentrated and precipitated in hexanes twice to provide **1** as a white solid (0.289 g, 86%). ^{1}H NMR (CD_3CN, 400 MHz): δ 7.30-7.18 (m, 12 H); 7.03 (d, *J* = 8.4 Hz, 2H); 6.94 (d, *J* = 7.4 Hz, 1H); 5.83 (d, *J* = 8 Hz, 1 H); 5.01-4.91 (m, 2 H); 4.63-4.58 (m, 1H); 4.31-4.26 (m, 1H); 3.18-2.95 (m, 3H); 2.74 (dd, *J*= 14.1, 9.7 Hz 1H). ^{13}C NMR (CD_3CN, 100 MHz): 172.8, 172.3, 156.8, 140.6, 138.4, 137.8, 134.8, 130.31, 130.25, 130.2, 129.32,

129.27, 127.7, 127.6, 120.0, 66.5, 57.1, 54.4, 38.4, 37.8. HRMS (ESI+) calculated for: $C_{26}H_{25}N_5O_5Na$: 510.1753, found: 510.1736. IR: υ_{max}/cm^{-1} 3301, 3029, 2109, 1697, 1658, 1531, 1506, 1256, 1040, 659.

Hydrogel preparation

A glass vial was used to carry out gel formation experiments. Compound **1** at different concentrations (0.1, 0.2, 0.3, and 0.5 wt%) was dissolved in DMSO and diluted with deionized water, and the critical gel concentration of compound **1** was found to be 0.5 wt%. Compound **1** (0.5 wt%) was dissolved in 50 µL of DMSO and then 950 µL of deionized water was added. The vial was left undisturbed for 20 minutes. Gel formation was tested by vial inversion method.

Hydrogel formation was also tested at various pH in PBS buffer (pH 7.4 and 6.5) and acetate buffer (pH 4.5). Compound **1** (2.5 mg) dissolved in DMSO (25 µL) was added to 475 µL of buffer (PBS or acetate), and the final pH was adjusted with dilute HCl and/or NaOH using a pH meter (S220 SevenCompact, Mettler Toledo). After adjusting the pH, hydrogel was left undisturbed overnight.

Visual hydrogel dissolution

A stock solution of TCO (2.5 mg) was prepared in 2 mL of PBS and used to make different dilutions. To hydrogel **1** (0.5 wt% in water; pH 3.4) was added 0.5 mL PBS containing TCO (1, 5 or 10 mM) followed by incubation at 37 °C. The hydrogel showed complete dissolution with 10 mM TCO by 4 h (Figure S5A). For the control experiment, to hydrogel **1** (0.5 wt% in water; pH 3.4) was added 0.5 mL PBS containing 10 mM CCO. After 24 h at 37 °C the gel did not show any sign of dissolution (Figure S5B).

To examine effect of pH on visible hydrogel dissolution, hydrogel **1** was prepared at different pH (7.4, 6.5 and 4.5) using PBS (for 7.4 and 6.5) and acetate (for 4.5) buffer. The final pH of hydrogel was adjusted using dilute HCl and and/or NaOH. TCO in PBS was added to the top of the hydrogels and incubated at 37 ℃. Visual gel-sol transition was monitored, a solution observed within 2-4 hours after addition of TCO (Figure S3).

Rheology

Rheology measurements were performed using a 40 mm parallel plate on an Oscillatory HR-3 Rheometer (TA Instruments) at 25 ℃. Compound **1** (5 mg) was dissolved in DMSO (50 µL) and after adding water (950 µL) the sample was quickly loaded on the rheometer and left undisturbed for 20 minutes to form a fibrous gel network. The linear viscoelstic region (LVER) measurements were done with 0.1 to 100% oscillation strain (Figure S14). The storage (G') and loss (G'') moduli were measured using dynamic frequency sweeps at a fixed strain of 0.5% in the frequency range 0.1 to 100 rad s^{-1}. For the time dependent rheology of hydrogel **1** with TCO (10 mM), 0.5 mL of TCO in water was added onto the gel (0.5 wt%) and rheology was measured at various time points in the dark at 25 ℃.

Transmission electron microscopy (TEM)

Transmission electron microscopy (TEM) was used to investigate the morphology of 0.5 wt% gels at pH 3.4 (water) and 7.4 (water adjusted to 7.4). The sample grids were prepared by depositing 10 µL of gel onto plasma-glowed TEM grids (300 mesh, carbon-coated copper grids). Excess sample was carefully removed after one minute using blotting paper. The grids were dried completely before viewing. They were viewed on a Philips CM100 TEM (Philips Electron Optics, Eindhoven, The Netherlands) operated at an accelerating voltage of 100 keV. Images were recorded using a MegaView 3 camera (Soft Imaging System GmbH, Münster, Germany).

Scanning electron microscopy (SEM)

The gel (0.5 wt%) sample was dried onto aluminum stubs overnight. After drying, the samples were sputter coated in an Emitech K575X Peltier-cooled high resolution sputter coater (EM Technologies Ltd, Kent, England). They were coated with 5 nm of gold palladium. Samples were viewed in a JEOL JSM-6700F field emission scanning electron microscope (JEOL Ltd, Tokyo, Japan) at an accelerating voltage of 5kV.

Infrared spectroscopy (ATR-FTIR)

Attenuated total reflectance-Fourier transform infrared spectroscopy (ATR-FTIR) was carried out using a Varian 3100 FTIR (Excalibur Series) instrument equipped with an attenuated total reflectance accessory (GladiATR, Piketech, USA). Following formation of the *p*-azidobenzyl carbamate hydrogel **1** (0.5 wt%), the sample was freeze dried (lyophilized) and the FTIR spectrum was measured (sample prior to trigger). TCO (10 mM) was added to the gel **1** (trigger experiment). Following an incubation period of 12 h (at 37 °C), the sample was lyophilized and re-analysed by FTIR.

For the time-dependent ATR-FTIR study, hydrogel **1** was prepared in different vials using PBS and incubated at 37 ℃ with 0.5 mL TCO (10 mM) in PBS. At the stated time points, the samples were lyophilized and analysed by ATR-FTIR.

For all FTIR measurements, the lyophilized gel sample was clamped directly on the ATR diamond crystal and spectra was recorded over a range of 400-4000 cm^{-1}. The spectrum was the mean of 64 scans with a resolution of 4 cm^{-1}. Data collected was analysed using Varian Resolution Pro, v4.1.0.101 software.

HRMS analysis of gel-sol transition

Hydrogel **1** was prepared using buffer (PBS and acetate) and adjusted using dilute HCl and/or NaOH to provide a final pH of 7.4 (PBS), 6.5 (PBS) and 4.5 (acetate). After adjusting the pH, TCO dissolved in PBS was added to the top of the hydrogel and samples were incubated at 37 ℃ for 12 h followed by lyophilization. The lyophilized samples were analysed by HRMS (ESI+ and ESI-).

HPLC kinetic release experiments

A 60 mM stock of TCO in PBS and a 10 mM stock of **1** in acetonitrile were used. To begin the 1,3-dipolar cycloaddition, 500 µL of the TCO stock was added to 500 µL of stock containing 10 mM **1**. The sample was incubated at 37 °C and at 20 minute intervals, an aliquot of 50 µL was injected onto the HPLC. The absorbance was measured using HPLC-UV at 254 nm (triplicate experiments).

For control experiments (run in triplicate); 500 µL of **1** stock was added to 500 µL of PBS and incubated at 37 °C. An aliquot of 50 µL was injected onto the HPLC at time intervals 0 min, 140 min and 24 hours.

Doxorubicin (DOX) release from dipeptide hydrogel 1

A 50 µL solution of dipeptide **1** (5 mg) in DMSO was prepared. In parallel, a 1 mg/mL stock solution of DOX in PBS was prepared and from this stock a 100 µL aliquot was diluted in 850 µL PBS. The PBS solution containing 100 µg/mL (0.17 mM) of DOX was added to the DMSO solution of **1**. The gel (0.5 wt% of **1**) was left undisturbed for 20 minutes. The gel was then washed with PBS (3 x 0.5 mL) to remove untrapped DOX.

Following this, 0.5 mL of *trans*-cyclooctenol (TCO, 5 mM) in PBS was placed over the gel and incubated at 37 ℃. For the control experiments *cis*-cyclooctenol (CCO, 5 mM) in PBS or PBS-only was added instead of TCO. At the indicated time-points (see Figure 3), 0.5 mL PBS was removed and replaced with the same amount of fresh PBS containing TCO (for controls

CCO or PBS-only). Care was taken so as to not disturb the gel. The absorbance of released DOX was measured with a plate reader (PolarStar Omega, BMG Labtech) at 485 nm. The cumulative percentage of DOX released was calculated from a standard curve of DOX in PBS measured at 485 nm (Figure S12).

Cell viability study

A stock solution of compound **1** (5 mg/mL) was made using DMSO (2.5%) in 1 mL of cell media followed by sonication to dissolve compound **1** completely. Different concentrations of **1** were prepared using the stock solution. Similarly, a stock solution of TCO (2.5 mg/mL) was prepared using cell media and different concentrations of TCO were prepared using the stock solution. Cells were plated at a density of 7.5 x 10^3 cells/well. Cells were incubated with compound **1** or TCO at different concentrations for 24 h, followed by addition of 10 µL of resazurin. After addition of resazurin, B16F10 melanoma and MDCK cells were incubated for 4 h at 37 °C. Fluorescence was measured at 544 nm (excitation) and 590 nm (emission) in a PolarStar Omega plate reader. Cell viability was normalized against cell only (100%) and cell-free controls (0%). Data were analyzed in GraphPad Prism.

Acknowledgements

This research was supported in part by a contract from the Health Research Council of New Zealand (A.B.G). The authors would like to thank the NMR and MS facility at the Department of Chemistry (Otago) and the Otago Centre for Electron Microscopy (OCEM) for allowing us to use their facilities, and the University of Otago (S.D.) and the Health Research Council (J.M.F.) for doctoral scholarships.

Keywords: click chemistry • peptide hydrogel • bioorthogonal chemistry • stimuli-responsive dissolution • drug delivery

1 (a) X. Du, J. Zhou, Shi, J., and B. Xu, *Chem. Rev.* **2015**, *115*, 13165-13307; (b) H. Shigemitsu and I. Hamachi, *Acc. Chem. Res.* **2017**, *50*, 740-750.

2 (a) J. Nanda and A. Banerjee, *Soft Matter* **2012**, *8*, 3380-3386; (b) C. K. Thota, N. Yadav and V. S. Chauhan, *Sci. Rep.* **2016**, *6*, 31167; (c) C. Ren, L. Chu, F. Huang, L. Yang, H. Fan, J. Liu and C. A. Yang, *RSC Adv.* **2017**, *7*, 1313-1317; (d) G. Liang, Z. Yang, R. Zhang, L. Li, Y. Fan, Y. Kuang, Y. Gao, T. Wang, W. W. Lu and B. Xu, *Langmuir* **2009**, *25*, 8419-8422; (e) S. J. Buwalda, T. Vermonden and W. E. Hennink, *Biomacromolecules* **2017**, *18*, 316-330; (f) W. Zhang, X. Zhou, T. Liu, D. Ma and W. Xue, *J. Mater. Chem. B*, **2015**, *3*, 2127-2136; (g) K. Basu, A. Baral, S. Basak, A. Dehsorkhi, J. Nanda, D. Bhunia, S. Ghosh, V. Castelletto, I. W. Hamley and A. Banerjee, *Chem. Commun.* **2016**, *52*, 5045-5048.

3 S. C. Bremmer, J. Chen, A. J. McNeil and M. B. A. Soellner, *Chem. Commun.* **2012**, *48*, 5482-5484.

4 (a) Z. Yang, G. Liang, M. Ma, A. S. Abbah, W. W. Lu and B. Xu, *Chem. Commun.* **2007,** 843-845; (b) X. M. Li, Y. Kuang, H. Lin, Y. Gao, J. F. Shi and B. Xu, *Angew. Chem. Int. Ed.* **2011**, *50*, 9365-9369.

5 (a) W. Liyanage, K. Vats, A. Rajbhandary, D. S. W. Benoit and B. L. Nilsson, *Chem. Commun.* **2015**, *51*, 11260-11263; (b) V. Jayawarna, M. Ali, T. A. Jowitt, A. F. Miller, A. Saiani, J. E. Gough and R. V. Ulijn, *Adv. Mater.* **2006**, *18*, 611-614.

6 (a) J. Li, Y. Kuang, J. Shi, J. Zhou, J. E. Medina, R. Zhou, D. Yuan, C. Yang, H. Wang, Z. Yang, J. Liu, D. M. Dinulescu and B. Xu, *Angew. Chem. Int. Ed.* **2015**, *127*, 13505-13509. (b) J. Li, J. Shi, J. E. Medina, J. Zhou, X. Du, H. Wang, C. Yang, J. Liu, Z. Yang, D. M. Dinulescu and B. Xu, *Adv. Healthcare Mater.* 2**017**, *6*, 1601400.

7 19. Y. Kuang, Y. Gao and Xu, B., *Chem. Commun.* **2011**, *47*, 12625-12627; (b) C. Colquhoun, E. R. Draper, R. Schweins, M. Marcello, D. Vadukul, L. C. Serpell and D. J. Adams, *Soft Matter* **2017**, *13*, 1914-1919; (c) A. D. Martin, J. P. Wojciechowski, A. B. Robinson, C. Heu, C. J. Garvey, J. Ratcliffe, L. J. Waddington, J. Gardiner and P. Thordarson, *Sci Rep.* **2017**, *7*, 43947.

8 H. Wang, D. Mao, Y. Wang, K. Wang, X. Yi, D. Kong, Z. Yang, Q. Liu and D. Ding, *Sci. Rep.* **2015**, *5*, 16680.

9 (a) Y. Zhang, H. W. Gu, Z. M. Yang and Xu, B., *J. Am. Chem. Soc.* **2003**, *125*, 13680-13681; (b) W. Liyanage and B. L. Nilsson, *Langmuir* **2015**, *32*, 787-799;

10 Y. Zhang, Z. M. Yang, F. Yuan, H. W. Gu, P. Gao and B. Xu, *J. Am. Chem. Soc.* **2004**, *126*, 15028-15029.

11 L. Chen, K. Morris, A. Laybourn, D. Elias, M. R. Hicks, A. Rodger, L. Serpell, A. J. Adams, *Langmuir* **2010**, *26*, 5232-5242.

12 C. D. H. Alarcon, S. Pennadam and C. Alexander, *Chem. Soc. Rev.* **2005**, *34*, 276-285.

13 M. Ikeda, T. Tanida, T. Yoshii and I. Hamachi, *Adv. Mater.* **2011**, *23*, 2819-2822.

14 R. Peltier, G. Chen, H. Lei, M. Zhang, L. Gao, S. S. Lee, Z. Wang and H. Sun, *Chem. Commun.* **2015**, *51*, 17273-17276.

15 R. J. Mart, R. D. Osborne, M. M. Stevens and R. V. Ulijn, *Soft Matter* **2006**, *2*, 822-835.

16 (a) F. B. A. Yu, P. Li, P. Song, B. S. Wang, J. Z. Zhao and K. L. Han, *Chem. Commun.* **2012**, *48*, 2852-2854; (b) J. Furne, A. Saeed, M. D. Levitt, *Am. J. Physiol. Regul. Integr. Comp. Physiol*, **2008**, *295*, R1479-R1485.

17 E. M. Sletten and C. R. Bertozzi, *Angew. Chem. Int. Ed.* **2009**, *48*, 6974-6998.

18 (a) J. A. Prescher and C. R. Bertozzi, Chemistry in living systems. *Nat. Chem. Biol.* **2005**, ***1***, 13-21; (b) N. K. Devaraj, R. Weissleder and S. A. Hilderbrand, *Bioconjug. Chem.* **2008**, *19*, 2297-2299.

19 J. Li, and P. R. Chen, *Nat. Chem. Biol.* **2016**, *12*, 129-137.

20 K. Neumann, S. Jain, J. Geng and M. Bradley, *Chem. Commun.* **2016**, *52*, 11223-11226.

21 (a) S. A. Fisher, A. E. G. Baker and M. S. Shoichet, *J. Am. Chem. Soc.* **2017**, *139*, 7416-7427; (b) H. Zhang, K. T. Dicker, X. Xu, X. Q. Jia and J. M. Fox, *ACS Macro Lett.* **2014**, *3*, 727-731; (c) P. E. Farahani, S. M. Adelmund, J. A. Shadish and C. A. DeForest, *J. Mater. Chem. B*, **2017**, *5*, 4435-4442; (d) V. X. Troung, K. M. Tsang, G. P. Simon, R. L. Boyd, R. A. Evans, H. Thissen and J. S. Forsythe, *Biomacromolecules*, **2015**, *16*, 2246-2253; (e) J. Xu, E. Feng, J. Song, *J. Am. Chem. Soc.* **2014**, *136*, 4105-4108; (f) A. Famili and K. Rajagopal, *Mol. Pharmaceutics*, **2017**, *14*, 1961-1968; (g) L. Xu, R. C. Cooper, J. Wang, W. A. Yeudall and H. Yang, *ACS Biomater. Sci. Eng.* **2017**, *3*, 1641-1653.

22 J. M. M. Oneto, I. Khan, L. Seebald and M. Royzen, *ACS Central Sci.* **2016**, *2*, 476-482.

23 (a) V. X. Truong, F. Li and J. S. Forsythe, *ACS Appl. Mater. Interfaces* **2017**, *9*, 32441-32445; (b) V. X. Truong, F. Li, F. Ercole and J. S. Forsythe, *Chem. Commun.* **2017**, *53*, 12076-12079.

10.1002/asia.201801184

24 S. S. Matikonda, D. L. Orsi, V. Staudacher, I. A. Jenkins, F. Fiedler, J. Y. Chen and A. B. Gamble, *Chem. Sci.* **2015**, *6*, 1212-1218.
25 S.S. Matikonda, J. M. Fairhall, F. Fiedler, S. Sanhajariya, R. A. J. Tucker, S. Hook, A. L. Garden and A. B. Gamble, *Bioconjugate Chem.* **2018**, *29*, 324-334.
26 R. van Brakel, R. C. M. Vulders, R. J. Bokdam, H. Grull and M. S. Robillard, *Bioconjugate Chem.* **2008**, *19*, 714-718.
27 Royzen, M., Yap, G. P., and Fox, J. M., *J. Am. Chem. Soc.* **2008**, *130*, 3760-3761.

10.1002/asia.201801184

WILEY-VCH

FULL PAPER

Entry for the Table of Contents (Please choose one layout)

Layout 1:

FULL PAPER

Click-to-dissolve: An alkene-azide click-reaction is used to promote hydrogel dissolution. The stable gel can encapsulate a cargo (e.g. doxorubicin) and upon addition of the strained alkene (a *trans*-cyclooctene), the click-reaction leads to gel dissolution and release of the encapsulated cargo.

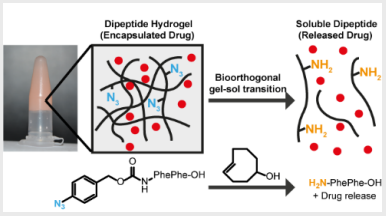

*Sumit Dadhwal, Jessica M. Fairhall, Shailesh K. Goswami, Sarah Hook, Allan B. Gamble**

Page No. – Page No.

Alkene-azide 1,3-dipolar cycloaddition as a trigger for ultrashort peptide hydrogel dissolution

Layout 2:

FULL PAPER

((Insert TOC Graphic here; max. width: 11.5 cm; max. height: 2.5 cm))

*Author(s), Corresponding Author(s)**

Page No. – Page No.

Title

Text for Table of Contents